

From fine sand to boulders: Examining the relationship between beach-face slope and sediment size

Nans Bujan^{a,*}, Rónadh Cox^b, Gerd Masselink^c

^a International Wave Dynamics Research Center, National Cheng Kung University, Tainan City 709, Taiwan

^b Geosciences Department, Williams College, Williamstown MA 01267, USA

^c Coastal Processes Research Group, School of Biological and Marine Sciences, Plymouth University, Plymouth, UK



ARTICLE INFO

Editor: Edward Anthony

Keywords:

Beach morphology
Gravel
Swash
Boulder ridges
Grain size
Beach-face slope

ABSTRACT

It is a long-standing maxim that coarser sediment sizes are associated with steeper beach-face slopes; but because most work has focused on sandy beaches, few data are available for the pebble, cobble, or boulder size ranges. Little is known, therefore, about how beach morphology and grain size relate at the coarser size grades. We compiled data from the literature—2144 measurements of beach-face slope with associated grain sizes—covering the range from very fine sand to boulders. This meta-analysis shows that beach faces do tend to steepen as average grain size increases, at least up to the cobble size range; but the trend is not simple. Although previous studies suggested a simple power-law relationship between grain size and beach-face slope, in fact the data distribution is best fit by a curve that is steep at the finer grain sizes but is much more gentle as grain size coarsens (and may trend downward for boulders). Fine and medium sands have the greatest range of reported slopes and the data support the importance of effective-weight modification and boundary layer dynamics as primary controls on beach-face steepness at these fine size grades. Around the very coarse sand size grade, a plateau marks a shift in beach dynamics: as hydraulic conductivity increases, beaches switch to being infiltration-dominated. The trend toward steeper slopes continues, but at a lower and steady rate, from granules through cobbles. There appears to be a falloff in slope for the coarsest boulder deposits (but we note that this is based on very few locations, so should be considered preliminary). The overall data distribution is described by a power-law function: $\tan \beta = a(D_{50} - 0.125)^b + c$. The broadness of each transition zone also shows that a range of factors, other than grain size, governs where that tipping point occurs. In the cobble and boulder size ranges there are two deposit categories: boulder beaches, and supratidal boulder ridges. Although not commonly thought of as beaches, boulder ridges record long-term storm deposition and reworking on the highest energy coasts. Supratidal ridges and boulder beaches seem to show different slope/grain-size relationships, with the steepest slopes occurring in boulder ridges, and with boulder beaches showing more gentle gradients than other coarse clastic beaches; but our data set reveals how little quantitative information exists about the coarsest end of the beach spectrum, and invites further work to investigate the sedimentology of cobble- and boulder-dominated systems.

1. Introduction

Beaches are the sand or gravel aprons that in many places form the interface between land and ocean. They extend inland to the limits of storm wave action, and offshore to the lower low water mark. The beach is always in flux, undergoing accretion or erosion depending on tidal regimes and the frequency of storms. The beach face is the part that interacts regularly with wave run-up and its shape can respond on short timescales, depending on the balance of forces moving sediment. Wave action—including wave impact, uprush, and backwash—is the

principal force controlling beach-face morphology (Bascom, 1951; Masselink and Short, 1993), but tidal currents, in/exfiltration, and wind action all combine to generate dynamic beach response (e.g., Elfrink and Baldock, 2002; Hartmann, 1991; Horn, 2006; Masselink et al., 2010; Turner and Nielsen, 1997).

Sediment grain size is a fundamental property of the beach. It is used for simple first-order classification (e.g., sand beach, cobble beach, boulder beach), but is also used to define beach states in a more sophisticated way (e.g., for conceptual models relating relative tide range and dimensionless fall velocity, as in Masselink and Short, 1993). Grain

* Corresponding author.

E-mail address: n-bujan@yandex.com (N. Bujan).



Fig. 1. Top: Wide sand beach in Warkworth, Northumberland, UK (photo by G. Masselink). Middle: Steep pebble beach in Slapton Sands, Devon, UK (Photo by J. Kelland, permission to reproduce given by the South West Coast Path Association). Bottom: Cobble beach in Westward Ho!, Devon, UK (photo by G. Masselink).

size also controls how beach morphology responds to the physical forcing factors given above (e.g., Bascom, 1951; Buscombe and Masselink, 2006; Wright and Short, 1984).

“The coarser the material, the steeper the beach” is a maxim of coastal geomorphology and engineering (Silvester and Hsu, 1997; Zenkovich and Zenkovich, 1967), and for grain sizes in the sand range ($0.0625 < D_{50} \leq 2$ mm), this trend is well established. Bascom (1951) first demonstrated the correlation between beach-face slope and the median diameter of sand, and it has been verified and quantified by subsequent workers, who have also expanded our understanding of nuances in the relationship (e.g., Boon and Green, 1988; Dubois, 1972; Holland and Elmore, 2008; Jennings and Shulmeister, 2002; Masselink and Li, 2001; McLean and Kirk, 1969; Reis and Gama, 2010; Sunamura, 1984). These studies have given rise to a range of formulae relating beach-face slope to some measure of grain size (e.g., Boon and Green, 1988; Kim et al., 2014; Reis and Gama, 2010; Soares, 2003; Sunamura, 1984; Vousdoukas et al., 2013). Across the board, however, these studies, and the quantification of controls on beach-face slope, have been largely based on sand beaches.

There are few studies of gravel beaches, and at the coarsest end of the spectrum, boulder-dominated systems ($256 < D_{50} \leq 4096$ mm) are the least studied of all (Paris et al., 2011). But there are sufficient data to show that gravel beaches tend to be steeper than those made of sand, with slopes often exceeding 10° ($\sim \tan \beta > 0.18$) (Buscombe and Masselink, 2006); and boulder-beach slopes can be greater than 15° ($\sim \tan \beta > 0.27$) (Etienne and Paris, 2010). Carter and Orford (1993)

pointed out that coarse clastic beaches have their own sedimentologic niche and characterised them as having, in general, steeper slopes than their sandy counterparts. Bluck (1998) agreed, but also emphasised the internal complexity of gravel beaches and the variety of ways in which they can form, some of which lead to differing slope characteristics. Jennings and Shulmeister (2002) found that pebble beaches ($2 < D_{50} \leq 64$ mm) in general had steep slopes, but that the slope varied depending on the extent to which sand was incorporated; and Buscombe and Masselink (2006) found that hydraulics, especially infiltration-driven processes, were more important in the morphodynamics of gravel beaches. Thus, there is some reasonable expectation that the slope/grain-size trends established for sand beaches might be extrapolated to gravel ones, but also the sense that the extrapolation would not necessarily be linear or simple, because of differing hydrophysics at the coarse clast sizes. These hypotheses, have, however, never been tested.

Because steepness influences the dynamics of up-rush and backwash, and consequently sediment concentration and transport, it is of primary concern for engineers. It is a key parameter in many engineering formulations, e.g., surf scaling and surf similarity parameters (Battjes, 1974; Guza and Inman, 1975). Beach-face slope is also related to attributes such as tourist perception of the beach (Phillips and House, 2009), coastal property values (Gopalakrishnan et al., 2011), species abundance (McLachlan and Dorvlo, 2005) or legal boundaries (Morton and Speed, 1998). A generalised understanding of the relationship between slope and grain size, across the full size spectrum, is therefore of value.

We conducted a meta-analysis of published data to create a unified overview of the relationship between grain size and beach-face slope, and in particular to examine the extent to which the existing formulae linking slope to size (which are based on sandy beaches) hold for coarse clastic beaches. The value of this analysis is that it creates a framework relating a wide range of beach deposits, and provides a generalised equation that describes the grain-size/slope distribution over the full range of beach grain sizes.

2. What exactly is the ‘beach face’?

The term ‘beach face’ is ubiquitous in coastal science. There is some variation in how the term is applied (McGlashan et al., 2005, and refs. therein; Bird, 2011). But most usages converge on the area between the low tide mark and the uppermost reach of high-tide wave run-up (Jennings and Shulmeister, 2002; Masselink and Li, 2001; Reis and Gama, 2010). Representative definitions include “the zone between the mean low water level and the seaward berm, which is equivalent to the upper limit of wave uprush at high tide” (Karsten, 2017) and “the seaward slope of the beach between the low tide line and the upper limit of wave swash” (Schwartz, 2006).

The definitions are clear enough, but—as anybody who has worked in the beach environment knows—it is difficult in the field to draw a line definitively demarcating the beach-face extent. Operationally, therefore, the mapped width of the beach face at any given site generally depends on the investigator’s estimate of the upper limit of run-up. In the case of beaches with simple slopes (e.g., Fig. 1), this is usually straightforward, as features such as the back-beach erosional scarp or vegetation line will show the limits of storm-wave action, and single berms reveal the most recent frequent high-water levels (Morton and Speed, 1998). It can be more complicated where there are multiple berms, each corresponding to a different run-up elevation with a

different return period (e.g., Fig. 2). In that case, the most common practice is to measure the beach up to the highest berm (e.g., Almeida et al., 2014; Bertoni et al., 2013; Pérez-Alberti et al., 2012).

3. The coarse end of the beach spectrum: boulder beaches and boulder ridges

Two distinct kinds of beach deposits characterise the coarse-grained end of the spectrum: boulder beaches and boulder ridges. These are the most under-studied of coastal deposits (cf. the small number of studies we were able to find for these deposits: Table 1). Therefore, differences and similarities among them require some systematic explanation.

Boulder beaches (Fig. 3, top) are the obvious coarse-grained analogues of sandy or pebbly beaches: intertidal deposits that form an unbroken sediment cover from the highest part of the foreshore through the subtidal zone. Being adjusted to high-energy waves that are competent to move the constituent clasts, they may not respond to fair weather swash and backwash; but some portion of the boulder beach is awash on a daily basis, and the full beach is active during storms (e.g., Etienne and Paris, 2010; Lorang, 2000; Oak, 1984).

But there is another, less familiar kind of beach deposit that forms above the high-tide line along very high-energy exposed coastlines with strongly negative sediment budgets: boulder ridges, also referred to as coastal boulder deposits (CBD) (Cox et al., 2018, 2012; Etienne and Paris, 2010; Nott, 2003; Paris et al., 2011). These supratidal boulder ridges occur only along rocky coasts with exposure to deep ocean water, where they mark the landward extent of storm-wave sedimentation (Fig. 3, bottom). Boulder ridges differ from boulder beaches in that they accumulate above the fair-weather high water mark, and in contrast to all other beach-type deposits, they do not form a continuous sediment blanket through the intertidal zone. Instead, they are separated from the water either by a bare rock platform or a cliff.

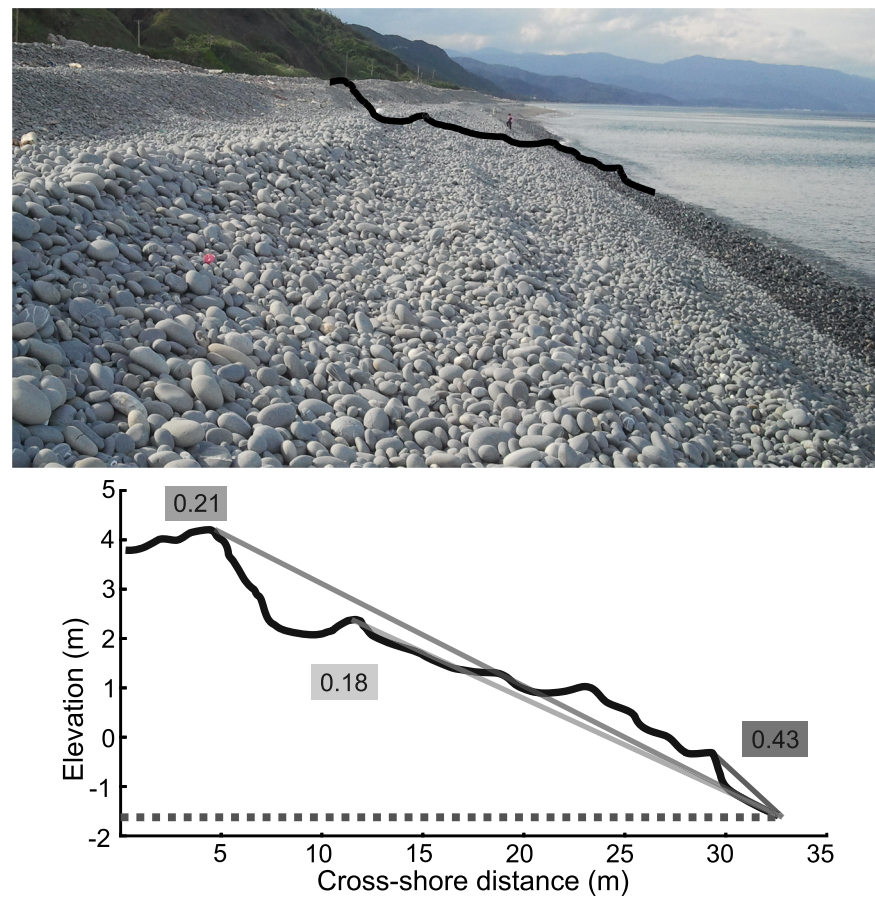


Fig. 2. Top: Steep cobble beach face incorporating many berms in Nantian, Taiwan (photo by N. Bujan). The profile shown in the bottom panel is indicated with a black line. Picture and profile were collected in May 2014. Bottom: Cross-shore topographic profile. Beach-face slope values are indicated for parts of the beach with different return periods of active run-up: hours ($\tan \beta = 0.43$, $\sim 23^\circ$), weeks ($\tan \beta = 0.18$, $\sim 10^\circ$), and years ($\tan \beta = 0.21$, $\sim 12^\circ$). This shows the level of complexity in some beach faces, and illustrates the difficulty of choosing a single slope value to characterise the beach face as a whole.

Table 1

Summary of the beach-face slope vs sediment-size data compiled. MDA is the median absolute deviation. Power law fit b is the value of b when a function $\text{Slope} = aD_{50}^b$ is fitted to the population. Details of references used are available in Bujan et al. (2018b).

Size category	Size range (mm)	Source studies number (and %)	Data points number (and %)	Median slope (and MDA)	Power law fit b	Power law fit R^2 (and p-value)
Sand	0.063–2	39 (50.0)	1695 (79.0)	0.08 (0.035)	0.68	0.32 ($9e^{-146}$)
Granule	2–4	3 (3.8)	77 (3.6)	0.12 (0.023)	0.60	0.13 (0.00155)
Pebble	4–64	24 (30.8)	244 (11.4)	0.16 (0.043)	0.16	0.10 ($8e^{-7}$)
Cobble	64–256	9 (11.5)	95 (4.4)	0.23 (0.066)	0.12	0.01 (0.244)
Boulder	256–4096	3 (3.8)	33 (1.5)	0.17 (0.029)	-0.68	0.30 (0.00104)
All	0.063–4096	78 (100)	2144 (100)	0.09 (0.042)	0.25	0.38 ($3e^{-227}$)



Fig. 3. Top: Boulder beach at the Burr, Shetland, UK (photo by R. Cox). Beach-face slope is 0.25 (14°) and $D_{50} = 270$ mm. Bottom: Boulder ridge on Inishmaan, Aran Islands, Ireland (location 54 in Cox et al. (2018); drone image by Peter Cox). The largest boulder in the field of view (above and to the right of the person in the blue jacket) has dimensions $10.4 \times 2.7 \times 0.6$ m and weighs approximately 43 t. The base of the boulder ridge is 19 m above the high water mark, and 220 m inland. Note that the bedrock platform is bare of sediment, and the boulder accumulation is not graded to the ocean. (For interpretation of the references to colour in this figure legend, the reader is referred to the web version of this article.)

Nonetheless, boulder ridges are thought of as beaches: formed by waves and adjusted to a wave climate, albeit the upper end of the local storm wave spectrum (Cox et al., 2018, 2012; Hall et al., 2006; Hansom and Hall, 2009; Paris et al., 2011; Williams and Hall, 2004). They are not common: they require specific geomorphic conditions that are

found in relatively few places (Cox et al., 2018; Hansom et al., 2015; Paris et al., 2011). But proof that they represent a component of the beach spectrum can be seen in places—e.g., the northeastern coast of Inishmaan, Ireland (53.090923; –9.564134)—where sandy beaches transform to boulder beaches, which then grade into boulder ridges as



Fig. 4. Temporal increase of sediment size and slope on the beach face of a sand-starved beach in Daren district, Taiwan (photos by N. Bujan). Visual estimations of the beach-face slope and the median grain size are indicated. The storm symbol between two photographs separates pictures taken just before (left) and after (right) the impact of a Typhoon.

the wave climate and geomorphology shift along a single continuous stretch of coastline.

Workaday waves do not reach them, but during storms—which, in effect, elevate the ocean surface and translate it inland—boulder ridges become the swash zone (e.g., Autret et al., 2016; Cox et al., 2017, 2012; Hansom et al., 2008). Their ocean-facing slopes are therefore the beach face during these events. The traditional definition of beach face, starting from the mean low tide level (e.g., Jennings and Shulmeister, 2002; Masselink and Li, 2001; Reis and Gama, 2010), is based on the assumption that the beach is graded through the intertidal. For boulder ridges, the intertidal shifts inland with storm surge. Therefore the storm beach-face slope can be measured as the angle from the ridge crest to the abrupt slope break at the toe of the ridge (Fig. 3, bottom).

Reliance on large storm waves for activation means that boulder ridges are built, reworked, and eroded on a continuous but punctuated basis, which is also consistent with the beach continuum. The large range of beach grain sizes—there are five orders of magnitude between fine sand and medium boulders ($\sim 0.06\text{--}600\text{ mm}$)—includes an implicit adjustment-timescale spectrum: sandy or pebbly beaches respond to gentle wave action, adjusting on timescales of hours or days. Cobble beaches require higher energy, and therefore will restructure over seasons or years. Boulder beaches and boulder ridges develop and change on timescales of years, decades or centuries, depending on the clast size and local wave climate.

The median clast size of boulder ridges is not always as large as the name would suggest. Boulder ridges are so called because they are

visually dominated by their largest clasts (Fig. 3, bottom), which can be tonnes to tens of tonnes in mass. The very open framework structure facilitates a sieving effect, however, so that finer clasts percolate into cavities while the largest clasts predominate at the surface, creating an appearance of boulder dominance. These environments can host individual clasts that are much larger than the boulders usually found on boulder beaches (e.g., Cox et al., 2018, 2017; Deguara and Gauci, 2017; Hansom et al., 2008; Hoffmann et al., 2013; Morton et al., 2008; Shah-Hosseini et al., 2016; Williams and Hall, 2004), but systematic clast counts (Cox et al., 2017; Jahn, 2014; Zentner, 2009) reveal that in fact these poorly sorted deposits have median grain size more commonly in the cobble range ($64 < D_{50} \leq 256\text{ mm}$). They are generally less well rounded than boulder beaches, but there is a distinct gradient in activation frequency, with less coarse ridges closer to sea level showing evidence for more frequent activation and greater rounding and sorting (Cox et al., 2017, 2012).

4. Methods

We extracted data from published studies, reports, and theses in which both grain size and beach profile measurements were included. The compiled data set comes from 78 sources (mostly published studies), and has 2144 entries (available in Bujan et al., 2018b). The studies are of different scales (some are local, some are international); and the number of transects in each study varies likewise (from 1 to 212). But each slope/grain-size data pair represents a single beach-face

transect, and thus each represents the hydrodynamic characteristics at the time and location of the data collection.

4.1. Grain size

There is no universal method for measuring sediment size, and the sources we used—which varied in the problems they addressed, and kinds of data collected—present a wide range of approaches. For sandy samples, dry-sieving was the main method used to extract the size populations (e.g., McLean and Kirk, 1969; Mwakumanya and Bdo, 2007; Reis and Gama, 2010), but samples differed: in some cases they were collected from the surface sediment layer (e.g., Reis and Gama, 2010), whereas in others cores were taken, to integrate across multiple layers (e.g., Mwakumanya and Bdo, 2007). Most of the studies collected point samples at specific locations, but some amalgamated sediment from several points on the beach to generate a composite sample (e.g., Pérez-Alberti et al., 2012). For coarser populations, where sieving was not possible, point-count techniques were the norm, either grid-based (e.g., Oak, 1984), or ribbon counts (e.g., Zentner, 2009).

Different methods of size data collection yield different results that generally need to be understood, and corrected for, if the data are to be directly comparable (Graham et al., 2012). In a meta-analysis of this sort, however, uncertainties related to methodology differences are subsumed by the noise in this complex natural system, where grain size can vary not only from site to site but also in time at any given site (e.g., Fig. 4). Sediment size variation can respond on the scale of a swash event (Blenkinsopp et al., 2011), a tidal cycle (Reniers et al., 2013), months (Aragonés et al., 2015), or a season (Prodger et al., 2016). In this context, we rely on the compilation of thousands of individual measurements, to integrate across all the sources of variability and reveal first-order relationships.

Representative grain size values were read from tables, pulled from descriptive text, or extracted from graphs. As far as possible we used median diameter (D_{50}) to represent population grain sizes. We accepted means (where reported instead of medians) in four cases, where raw data were not provided and we could not compute our own median values. As the data set ranges over several orders of magnitude, and there is great inherent variability in the underlying populations, errors associated with using mean instead of median in these cases is considered insignificant relative to the scale of variation and noise in the data set as a whole.

4.2. Beach-face slope

Beach-face slope is commonly characterised by a single value, generally representing the hypotenuse of a right-angle triangle pinned by the beach crest and the low water mark (Jennings and Shulmeister, 2002; Qi et al., 2010; Reis and Gama, 2010; Soares, 2003). For simple beaches, where the face is approximately planar, this approach is well established as a sufficiently good approximation (e.g., Fig. 1; Aagaard et al., 2012; Almeida et al., 2013; Ivamy and Kench, 2006). However, in the many cases where the beach profile is not a straight line from the highest point of the subaerial beach to the low tide water level, choosing how to characterise its slope is not straightforward. Examples are concave or convex beaches (Karunaratna et al., 2012; Masselink et al., 2009; Mwakumanya and Bdo, 2007), beaches that include scarps (Fig. 5, top; Qi et al., 2010), and beaches that have multiple berms (Fig. 2; Fig. 5, middle; Carr, 1969; Dail et al., 2000). Some beaches are composite, with, for example, a gently sloping finer forebeach and a steeper coarser backbeach (Fig. 5, bottom; Borzone and Rosa, 2009; Carter and Orford, 1993; Isla and Bujalesky, 2005; Jennings and Shulmeister, 2002). In these cases, different parts of the beach face can be simplified as separate straight-line segments (Fig. 2; Isla and Bujalesky, 2005), as has been done in a number of the studies in our data set.

The slopes found in our review were measured in a variety of ways,

from simple cross-beach measurements with Abney level (e.g., McLean and Kirk, 1969), dumpey level (e.g., Mwakumanya and Bdo, 2007) or theodolite (e.g., Anfuso et al., 2007), to detailed topographic profiles constructed either using traditional surveying methods (e.g., Roberts et al., 2013) or using modern technologies such as laser scanners (e.g., Almeida et al., 2013) or UAV photogrammetry (e.g., Pérez-Alberti and Trenhaile, 2015a). Many papers with grain-size data included surveyed beach profiles, so although slopes might not have been calculated as part of those studies, we were able to extract them from the topographic data. In all cases we made sure to pair the grain-size data with slope values from the specific transects on which they had been measured. We report the slopes both as gradients ($\tan\beta$) and in degrees.

4.3. Structure of the data set

We accessed only a fraction of the available studies on sandy beaches, and yet that portion of the graph is dense with data: a testament to the vast amounts of work done in those environments. For pebble beaches there were fewer studies, but we searched diligently and included all available. In the cobble and boulder ranges we struggled to find data. We extended the net across as many databases as possible, and believe that we have gathered most if not all of the available publications.

As is the case with most meta-analyses, our data set integrates across a wide range of sampling strategies and measurement techniques. The number of data included in each size-population count is variable, ranging from a few tens of grains to a few thousand. The slope data likewise vary, from cross-beach sightings that yield a single slope value representing the topographic difference between the beach crest and the water's edge, to high-precision LIDAR-based profiles from which exact measurements of segments can be derived. Error bars for individual data points on the graph cannot therefore be calculated. But the beauty of data sets that stretch across several orders of magnitude is that the errors on individual points pale in comparison to the scale of the natural variation in the system: in this case the slope values and grain sizes range across two and five orders of magnitude, respectively. And with more than two thousand beach profiles represented on the graph, with many grains counted on each profile, we expect that the overall trends are robust.

5. Results

The relationships between grain size and beach-face slope are shown in Fig. 6, covering grain populations with median sizes from 0.07 mm (very fine sand) to 770 mm (medium boulder per the expanded Wentworth size scale of Terry and Goff, 2014), and slopes ranging from 0.01 (0.6°) to 0.83 (40°). There are 2144 data points from 78 published studies (Table 1). The data are noisy, which is to be expected given both the amount of variability in beach systems and the wide range of data sources; but an overall power-law tendency toward steeper slopes with increasing grain size is evident. Equally clear is the complexity of the trend, as the shape of the distribution changes across the grain size spectrum.

The dependency is strongest at the finest sizes, with a steep slope through fine to medium sand. For coarse sand and beyond, average slope continues to increase, but at a slower rate (Fig. 7). For the coarsest size populations, in the boulder size range, the pattern is less clear. Slopes may decrease in this size range; but a paucity of data, and problems related to data comparability (which will be discussed in Section 8.4.3), mean that we cannot make any firm interpretations of trends for the coarsest grained beaches. Two things are clear, however, and both will be discussed below in detail: first, the general trend toward increasing beach-face steepness with coarser grain size is shown to be true across the full range of beach types; and second—in contrast to previous interpretations—the power-law relationship is not simple.



Fig. 5. Top: Narrow sandy beach face displaying a recent erosion scarp in Nags Head, USA (photo by D. Lindbo). Middle: Complex mixed sand and gravel beach in Daren, Taiwan (photo by N. Bujan). Bottom: Composite sand and gravel beach in Daren, Taiwan (photo by N. Bujan), displaying a steep coarse foreshore ($\tan \beta \sim 0.6$, $\sim 31^\circ$) and a milder sandy low-tide terrace ($\tan \beta \sim 0.15$, $\sim 9^\circ$).

5.1. Sand-dominated beaches

Sand beaches account for the majority of available measurements: 79% of all values in our data set are in the sand size category. Beaches constructed of very fine sand ($0.0625 < D_{50} \leq 0.125$ mm) are rare, so at this lowest end of the size spectrum there are only 14 values in our data set. In contrast, the fine sand category ($0.125 < D_{50} \leq 0.25$ mm) and medium sand category ($0.25 < D_{50} \leq 0.5$ mm) contain 403 and

812 values respectively. Overall, 57% of all data come from fine to medium-grained and 22% from coarse ($0.5 < D_{50} \leq 1$ mm) to very coarse ($1 < D_{50} \leq 2$ mm) sand beaches (Table 1).

The sand category includes the lowest slopes of all environments: 0.02–0.04 medians in the very fine and fine sand grades (Fig. 7). The lowest values, which are close to flat (< 0.01 , or $< 0.5^\circ$), almost all occur in sands finer than 0.3 mm; and slopes less than 0.03 (2°) are all found in sand finer than 0.6 mm (Fig. 6). Slopes within the fine to

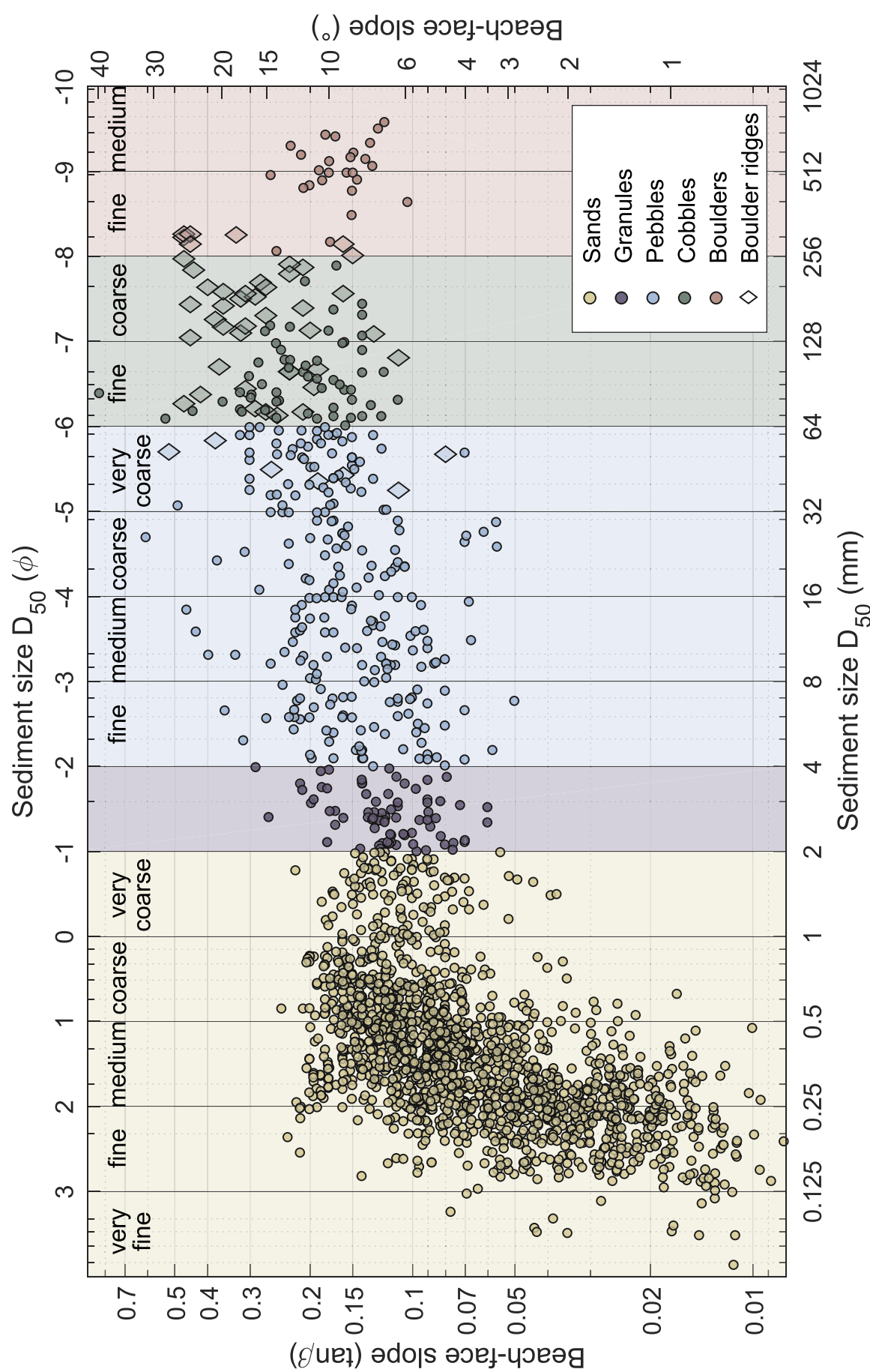


Fig. 6. Log-log plot of beach-face slope versus median grain size. Data gathered from published studies (see Bujan et al., 2018b). Panel and symbol colours correspond to sediment-size categories. Size grades (see Terry and Goff, 2014) are indicated and boundaries are given in mm on the lower and in ϕ on the upper X axis. Diamonds indicate data from supratidal boulder ridges (note that boulder ridges are so named because they are visually dominated by the largest clasts; in many cases their average grain sizes, when measured, are smaller than the name would suggest).

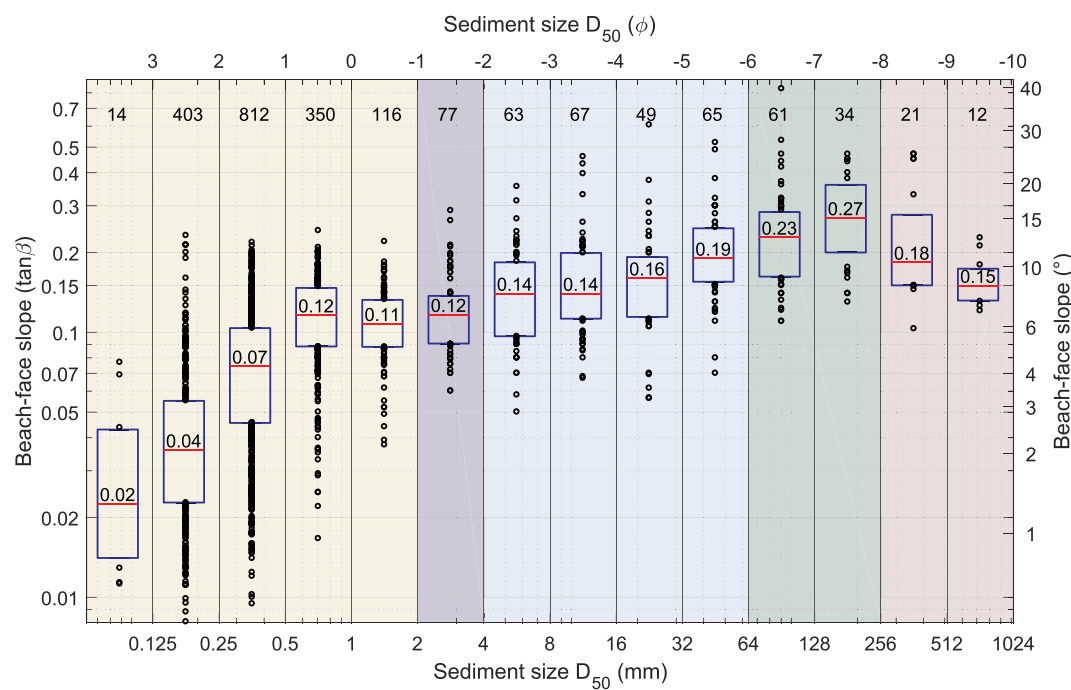


Fig. 7. Box plots of beach-face slope values regrouped by sediment-size grades. Red line indicates the median. Bottom and top edges indicate 25th and 75th percentiles respectively and black circles show other values. The number of data points and the median value per size category are indicated on top of and inside boxes, respectively. (For interpretation of the references to colour in this figure legend, the reader is referred to the web version of this article.)

medium-grained sand populations sprawl across the range 0.01–0.25 (~0.5–14°). These size grades have the greatest range in reported slopes. There is a noisy but statistically significant ($p < 0.0001$) trend, which is revealed more clearly in the binned data (Fig. 7): median slope increases from 0.04 to 0.07 (~2–4°) as grain size coarsens from fine to medium sand.

From coarse to very coarse sands, there is a slight decrease in both median and steepest slope values (Fig. 7). This is not statistically significant, however, and corresponds also to a decrease in data density: there are far fewer available studies of coarse than of fine or medium sand beaches (Fig. 6). Among 1695 data points collected in the sand size range, only 15 have a slope greater than 0.2. Therefore a steepness of approximately 0.2 (in the region of 10°) can be considered a universally relevant upper limit of sandy beach-face slopes.

5.2. Granules, pebbles, and cobbles

Data-point density is low above 2 mm (Fig. 6), reflecting the much smaller number of studies available (Table 1). Although the data are noisy, there are demonstrable trends: values in the granule to cobble size range display the least complex behaviour of our analysis with a steady increase of beach-face slope with grain size. Median slope increases from 0.12 (~7°) for granules ($2 < D_{50} \leq 4 mm) to 0.23 (~13°) for cobbles. Also, all slopes exceed 0.05 (~3°): there are no ‘flat’ beaches in these environments. Cobble beaches are hosting the steepest beach faces with a maximum slope of 0.83 (~40°) and no value smaller than 0.11 (~6°). In the fine cobble range, most data come from regular beaches (Allan et al., 2005; Bujan et al., 2018a; McKay and Terich, 1992). The coarse cobble range is the steepest of all size grades; the median slope is 0.27 and there are few values for regular beach faces: most of the data comes from boulder ridges studies (Jahn, 2014; Zentner, 2009).$

5.3. Boulders

Boulders are by far the most understudied sediment class in the coastal environment. There has been a recent surge in studies dedicated

to coastal boulder deposits (e.g., Autret et al., 2016; Cox et al., 2018, 2017, 2012; Kennedy et al., 2017; Nott, 2003; Williams and Hall, 2004), but most have focused on characteristics of individual boulders (position, shape, mass, etc.) rather than on broader sedimentologic parameters. Therefore there are very few available studies incorporating both clast-size distributions and profile data since the classic—almost the only—systematic work on boulder beaches of Oak (1981, 1984): this size range is the most poorly populated part of the distribution with only 33 data points (less than 2% of the data).

Deposits with $D_{50} > 256$ mm have slopes ranging from 0.10 to 0.48 (~6–26°) with a median of 0.17 (10°). The slope range for boulder beaches (excluding data from boulder ridges) is 0.1 to 0.3 (~6–17°). The limited data means that we have not captured the full range of likely slopes for boulder beaches and boulder ridges. It is possible that the slope/size dependency reverses for boulder beaches (Fig. 6), but this is statistically weak.

6. Evaluating the data set: comparing trends at the level of individual studies

We can test whether the overall trend in the amalgamated data set is representative and meaningful by considering the referenced studies separately. Fig. 8 shows slope/size correlations for the most robust studies in the database (i.e. we excluded those with less than 10 data points, or for which the range of median sizes was less than 1 ϕ). We then fitted a power law to each set ($Slope = aD_{50}^b$). If beach-face slope is related to grain size, and if the slope of the dependency changes for coarser populations, then we should see these tendencies in the different subsets of the main data pool.

The general tendency for slope to increase with increasing median size is clearly borne out, as are the observations that the relationship is strongest among sandy beaches, where many studies have high b values ($0.5 < b < 1.5$). Steepness increases more gradually at coarser grain sizes: for granules and pebbles, b values are mostly < 0.5 . Complications in the cobble and boulder ranges and possible reversal of the grain-size/slope relationship at these coarsest clast sizes are also evident in this diagram. Each of these aspects will be discussed below.

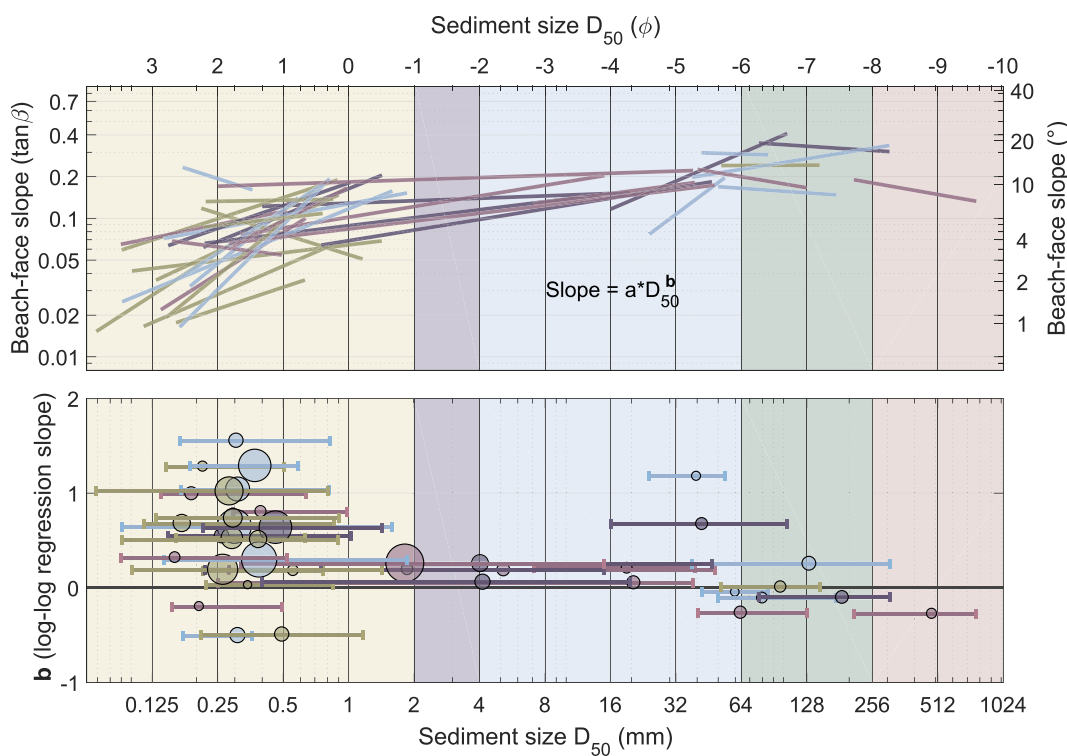


Fig. 8. To test whether the grain-size/slope relationships seen in the data set as a whole can be recognised at the scale of specific sites or regions, we show here regression analyses for individual studies in the database. We excluded studies with too few points, or which covered too narrow a range of grain size to be meaningful. So each line on this plot represents a single study with more than ten data points, and covering a size range greater than 1ϕ . The data are fitted by a power-law function of the form $Slope = aD_{50}^b$. The top panel shows the lines of fit on a log-log scale and bottom figure displays the slope exponent b as a function of the median sediment size in each study (circle). Bars indicate the grain size range and circle size is proportional to the number of data points. (For interpretation of the references to colour in this figure legend, the reader is referred to the web version of this article.)

Among sandy beaches, only three data sets display a negative correlation, and these studies all reveal roles of other variables in controlling beach-face slopes. Data from Pinto et al. (2009) (personal communication, golden down-trending line on Fig. 8) come from various beaches with different locations. Data from Dubois (1972) (blue down-trending line on Fig. 8) represent situations where heavy-mineral concentrations vary on the beach face. In that study, the author demonstrates that slope angle is a direct function of the change in average specific gravity of the sediment: dense grains are hydrodynamically coarser than their quartz size equivalents, and finer grained sands rich in heavy minerals therefore hold steeper slopes than coarser, quartz-rich sands. Similarly, Borzone and Rosa (2009) (purple down-trending line in Fig. 8) present data from various beaches with unusually high concentrations of organic macrodetritus, and it seems likely that the multiple wrack-lines in those environments affect the sediment dynamics on the beach face. That these studies show different slope/size trends provides insight into the noise in the database, and highlights the fact that other variables cannot be ignored in understanding beach-face morphologies.

Data sets in the granule and pebble sand ranges all have positive b values. As in the amalgamated data (Fig. 6), the trends have shallower slopes than do sandy beaches. This is also the least variable part of Fig. 8, a number of the data trends being very close together, with a strong degree of overlap and little variation in the slope of the lines.

The coarsest populations—medians in the cobble and boulder ranges— are poorly represented: the data density is low (Fig. 6), and only six studies in this size range appear on Fig. 8. With the exception of Jahn (2014), which shows a positive b value (pale blue line on Fig. 8), these studies produce trends that are flat or slightly negative.

The fact that the data from individual studies show slope/size trends that match—in sign and in relative slope—the overall patterns in the

data set as a whole, validates the meta-analysis and the patterns it reveals.

7. Numerical description of beach-face slope as a function of grain size

Many researchers have proposed empirical relationships to predict beach-face slope, and a selection of popular or recent formulae from the literature is presented in Table 2. These expressions have several things in common. First, all include terms relating in some way to wave power: breaker height, significant wave height, or wave period. Second, most take sediment size into account via single power expressions of D_{50} , and so plot as straight lines on a log-log plot. And finally, these formulae have been calibrated using data from beach faces made of sediment not coarser than sand or pebbles.

To examine how well these formulae describe natural systems across the grain size spectrum, we plot them in relation to the amalgamated data set (Fig. 9, top panel). The equations of Flemming (2011) and Reis and Gama (2010) yield steep slope/size curves that fit well with the data from fine to medium sand beaches, but they deviate strongly from observations in coarse sand and above. In contrast, the formulae of Soares (2003), Rector (1954) and Kim et al. (2014), although quite different from each other in form (Table 2), produce very similar, near-parallel lines on Fig. 9. They succeed in describing the steady increase of slope within the granule to cobble size range, but fail to match the steeper trend shown by sand beaches. The Sunamura (1984) equation has a steeper trend that works for granules and pebbles, but deviates at both the finer and the coarser ends of the data distribution. Least successful are the relationships from Uda (1982) and Sunamura (1975), which cross the data distribution at a tangent, and are valid at best for a small segment in the medium sand to granule

Table 2

Formulae expressing beach-face slope as a function of sediment size. β : beach-face slope in degrees, Φ_{50} : median sediment size in ϕ units, $\tan \beta$: beach-face slope, c_1 , c_2 and c_3 : empirical coefficients, T : wave period, D_{50} : median sediment size in mm, L : wave length, H_s : significant wave height, H_b : breaker wave height, HTS: spring tidal range, BW: beach-face width. Wave-power effect is indirectly included in the Flemming (2011) equations as they are set up for reflective versus dissipative beaches. In Reis and Gama (2010), the coefficient c_1 was not specified and is given here an arbitrary value to fit data in the sand range.

Source	Equation	Comments
Flemming, 2011:	$\beta = 13.39 \exp(-\Phi_{50}/0.7954)$ $\beta = 0.057 + 33.5152 \exp(-\Phi_{50}/0.8517)$	For a dissipative beach state For a reflective beach state
Kim et al., 2014:	$\tan \beta = c_1 T^{c_2} D_{50}^{c_3}$	$c_1 = 0.332$; $c_2 = -0.416$; $c_3 = 0.122$
Rector, 1954:	$\tan \beta = c_1 (D_{50}/(1000L))^{c_2}/(H_s/L)^{c_3}$	$c_1 = 0.07$; $c_2 = 0.1$; $c_3 = 0.42$
Reis and Gama, 2010:	$\tan \beta = c_1 H_s^{c_2} D_{50}^{c_3}$	$c_1 = 0.9$; $c_2 = -\frac{10}{3}$; $c_3 = \frac{4}{3}$
Soares, 2003:	$\tan \beta = (\text{HTS} + H_b) \sqrt{D_{50}/c_1}^{0.25}/\text{BW}$	$c_1 = 1.03125 \text{ mm}$
Sunamura, 1975:	$\tan \beta = c_1 T \sqrt{g D_{50}} / H_b$	$c_1 = 0.10$
Sunamura, 1984:	$\tan \beta = c_1 (T \sqrt{g D_{50}/1000} / H_b)^{0.5}$	$c_1 = 0.12$
Uda, 1982 (cited in Voudoukas et al., 2013):	$\tan \beta = c_1 (D_{50}/(1000H_s))^{c_2}$	$c_1 = 4.5$; $c_2 = 0.5$

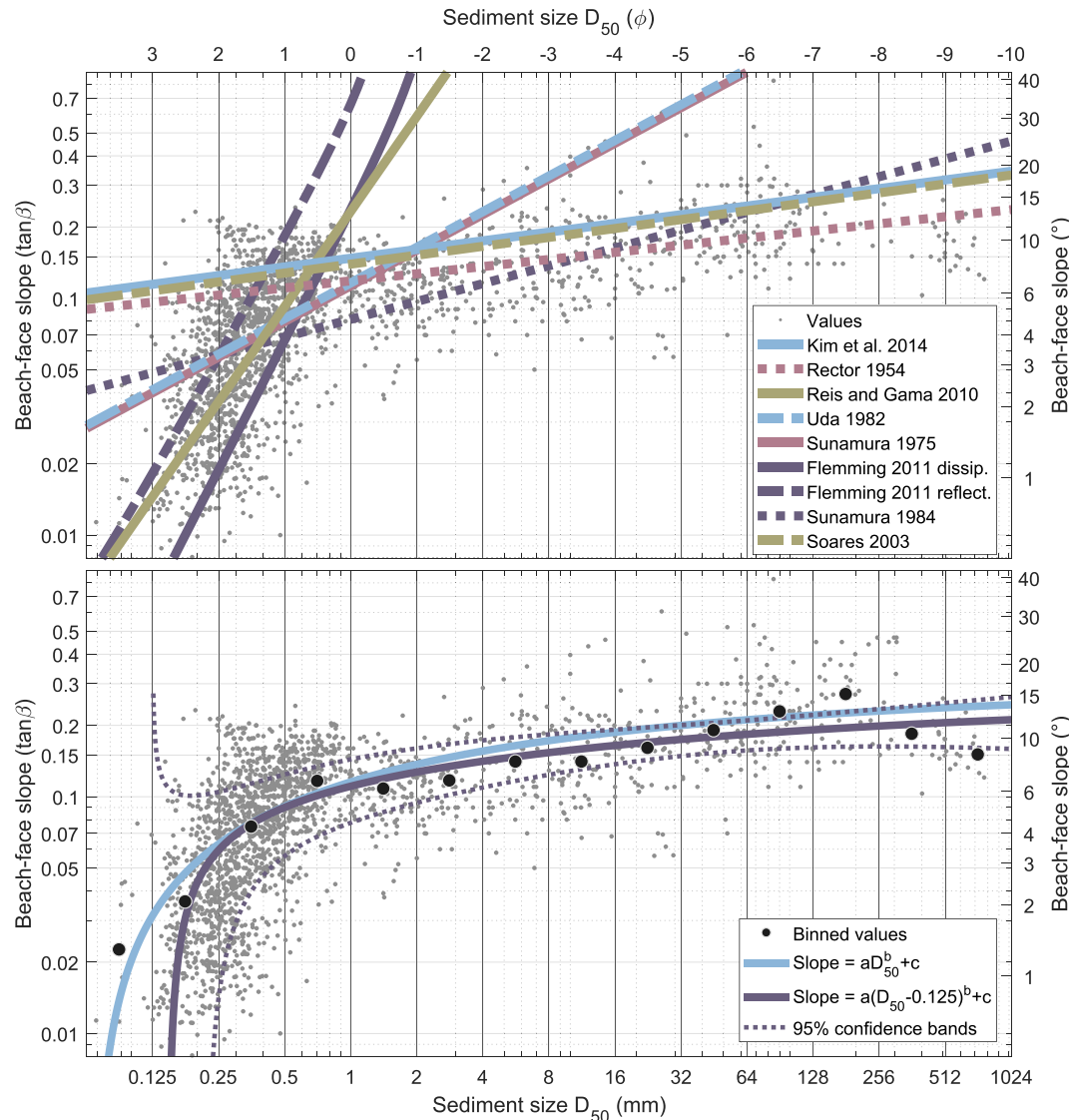


Fig. 9. Top: Plots of the beach-face slope equations presented in Table 2. The following parameters were used: $H_s = H_b = 1.5 \text{ m}$, $T = 7 \text{ s}$, $L = gT^2/(2\pi)$, HTS = 2 m, BW = 25 m. Bottom: Fit of Eq. (1) ($a = -0.178$; $b = -0.187$; $c = 0.294$) and Eq. (2) ($a = -0.154$; $b = -0.145$; $c = 0.268$) to the data binned in $1-\phi$ intervals. 95% pointwise confidence bands are indicated for Eq. (2). (For interpretation of the references to colour in this figure legend, the reader is referred to the web version of this article.)

range. The key point is that even the most representative of the equations cannot describe the full distribution of the data.

7.1. A new equation describes the data pattern across the full range of grain sizes

It is clear from Fig. 9 (top panel) that the data pattern cannot be characterised by a simple exponential or power-law function. To provide a model that accurately describes the shape of the distribution across the full slope-size spectrum we need to increase the numerical complexity; but because the data are noisy and the model is at best an approximation to reality, we also want to keep it as simple as possible. The simplest increase in complexity is to extend the power law to two terms of the form:

$$\tan \beta = aD_{50}^b + c \quad (1)$$

Fitting Eq. (1) to the data set (binned in $1-\phi$ intervals) generates a curve that is steep in the sand domain, rolls over to a much more gentle slope in the medium to coarse sand range, and tracks the central tendency through the pebble and cobble fields (pale blue line on Fig. 9, bottom). It is not fully adequate, however, as it doesn't capture the very steep slope increase in the very fine to medium sand range. To create a more realistic numerical description of the data distribution, we tied the grain size to an origin at 0.125 mm (the lower boundary of the fine-sand category), so that the equation becomes:

$$\tan \beta = a(D_{50} - 0.125)^b + c \quad (2)$$

The sole difference between Eqs. (1) and (2) is the location of the origin. Our rationale is hydrodynamic. Grains in the very fine sand or silt range generally cannot settle under wave action to form a beach face. Instead, such fine sediments form tidal flats and are only found in sheltered environments. Thus we restrict the equation to those grain sizes that are truly beach-forming. Eq. (2) (dark blue line on Fig. 9, bottom) accurately depicts the behaviour of fine-grained beaches, while being identical to the unmodified equation (within error) at coarser grain sizes.

We note that the curve is not well constrained in the coarse cobble to boulder zones, where data density is lowest. It is unclear whether the relationship continues with the same trajectory, or whether there is a downturn in characteristic slope at the largest clast sizes. That issue cannot be resolved by this data set, and points to the need for more study at the coarse end of the size distribution.

This unifying-equation approach is highly generalised, and far from perfect. The data are very noisy, and beach-face slope depends on many factors, of which size is only one. But Eq. (2) robustly represents the way that the dependency changes as grain size increases, from the very rapid rate of change across the sand range to the more gradual one at the coarser size grades.

8. Discussion

The integrated data set presented here takes a complex suite of dynamic environments and squeezes them into a single parameter space. It includes beach faces of all kinds, making no distinctions in terms of sorting, grading, or mixed beaches, ignoring whether the studied beaches are aggrading or eroding, taking no account of season nor variations in wave power. Clearly it's a simplification: the diversity of beach deposits generally resists description by single metrics such as median grain size (Holland and Elmore, 2008). And yet, viewed in this way, the data reveal distinct, statistically significant trends across widely differing systems and regimes. This may therefore be saying something fundamental about beach hydrodynamics, which may also point to avenues for fruitful further research.

In this section we discuss the data in more detail, stepping through the different sediment-size ranges and highlighting both our

interpretations and also those aspects that are either poorly constrained or puzzling.

8.1. Weak infiltration at small grain sizes may explain steep slope/size curve for fine sand

During each wave cycle, water percolates into and out of the beach face by infiltration and exfiltration (Packwood, 1983). Efficiency of these processes varies with grain size (also with sorting, but we will not address that aspect here). On fine-sand beaches in particular, permeability is impaired, and the amount of water exchange during a single uprush-backwash cycle is minimal (Turner and Masselink, 1998).

When grain size is so small that infiltration is ineffective—median less than about 0.5 mm, per Bagnold (1940)—water brought across the beach by swash uprush has to return during backwash. But the sloping beach surface causes differences in pressure gradients: during uprush, there is net downward pressure on the beach face, which reverses during backwash. This modifies the effective weight of particles, so that grains are ‘heavier’ during uprush and ‘lighter’ during backwash. In consequence, the upper layer of the beach is subject to destabilisation and offshore transport during backwash, which can flatten the beach profile over time (Butt et al., 2001).

The effective-weight effect, and hence the beach-leveelling tendency, is strongest for very fine and fine sands, and decreases dramatically with increasing grain size beyond that range (Butt et al., 2001; Hoque and Asano, 2007). This may explain the very low slope values ($\tan \beta < 0.05$, or $< 3^\circ$) that are observed for sands < 0.25 mm, and also the sharply increasing trend in the finest sizes (Figs. 6, 9). The effect is very sensitive to grain size below ~ 0.3 mm, while it is quasi-steady above (Butt et al., 2001). Such sensitivity—which presumably would also encompass subtle differences in local slope and sorting—could explain why the finest-grained beaches not only tend to steepen dramatically with increasing grain size, but also display such a wide range of slopes. The effective-weight effect may be enhanced in some cases, and overridden in others, generating very variable morphologic response in fine-sand beaches.

8.2. Onset of boundary-layer effects may drive the change in slope characteristics in the coarse to very coarse sand range

At $D_{50} \sim 0.5$ mm there is a marked shift in the data pattern on Fig. 6. The slope/size relationship levels off, and the minimum beach face slope increases abruptly: slopes lower than 0.03 ($\sim 2.5^\circ$) are not encountered past this point.

There is an opposite effect that exists concurrently to the effective-weight effect: as hydraulic conductivity increases, so do rates of infiltration and exfiltration during the uprush-backwash process (Masselink and Puleo, 2006), and these influence grain transport by their effect on boundary layer thickness. During uprush, water from the base of the flow seeps into the beach face, which thins the boundary layer and shifts faster-moving, more turbulent flow closer to the bed, enhancing the potential for sediment transport. Conversely, during backwash, water percolating out of the beach is added to the flow base, thickening the boundary layer, decreasing near-bed velocity, and protecting the sediment from turbulent vortices higher in the water column. The result is greater bed shear stress during uprush, promoting onshore sediment transport, which tends to increase beach-face slope (Butt et al., 2001; Turner and Masselink, 1998).

The grain size threshold at which boundary layer thickness effects—and consequently onshore transport—start to offset effective-weight effects is around 0.4–0.6 mm (medium to coarse sand) (e.g., Butt et al., 2001; Hoque and Asano, 2007; Karambas, 2003; Nielsen, 1998), which corresponds to the region on Fig. 6 where the minimum values for beach-face slope suddenly increase dramatically. We interpret this to reflect the onset of infiltration-driven hydrodynamics.

At these threshold grain size intervals, however, infiltration

dynamics are not yet dominant, and as the boundary-layer effect ramps up, the effective-weight effect (although diminishing) remains in force (Butt et al., 2001). The interplay of opposing forces in the coarse to very coarse sand range—the boundary-effect tending to increase beach-face slope, and the effective-weight effect tending to decrease it—may explain why the data pattern stays approximately flat through this interval (Fig. 6). There is no statistical difference between the median beach-face slopes for coarse and very coarse sand (Fig. 7), but there is a smaller spread in the values. In particular, the upper slope limit is lower, and there is a slight ‘necking’ of the distribution in the very coarse sand interval ($1 < D_{50} < 2$ mm). In part this may be an artifact of the data set, as the number of studies (hence data points) decreases with increasing grain size; but the fact that the inflection point corresponds to this critical threshold suggests that dynamics are at work.

8.3. Swash asymmetry dominates from the granule size range upward

Since the work of Bagnold (1940) it has been known that some grain size criterion separates infiltration-dominated beaches from those that are relatively impermeable to swash, and that the critical size interval is somewhere in the coarse sand to fine pebble range (0.5 to 9 mm). This change in the hydraulic conductivity of the beach—and the consequent losses in uprush volume due to swash infiltration—fundamentally alters the geomorphology of coarser beaches, driving them to steeper profiles.

Hydraulic conductivity of the beach, and consequently the quantity of infiltrating water, is related to grain size by a power law (Masselink and Li, 2001; Shepherd, 1989). The greater the permeability, the less the backwash strength and the less efficient the seaward transport of grains. The more powerful the swash relative to the backwash, the steeper the beach face; and as clast size coarsens in gravel beaches this power asymmetry becomes more pronounced. Because inhibition of backwash transport tends to promote steeper beaches, increasing beach-face slope with increasing clast size is therefore expected.

The efficiency of infiltration increases progressively as size (and sorting) and hydraulic conductivity increase through the sand ranges, and the effective-weight effect decreases in tandem. Eventually the threshold is fully crossed, and swash asymmetry dominates. Numerical modelling (Masselink and Li, 2001) indicates that a median grain size of 1.5 mm might be the critical size for this shift.

The distribution of data (Figs. 6, 7) indicates that this change probably occurs around the 2 mm sand-to-granule transition in natural systems: beyond 2 mm and up to the cobble range, slope tends to increase linearly with size on the log-log plot. This is fully consistent with the model of Masselink and Li (2001), which explicitly excluded pressure gradients, boundary layer dynamics, and only looked at the influence of swash infiltration losses. A key result of this study is that the data distribution illustrates the geomorphologic response of the beach to differing dynamical drivers over different grain size intervals. The break in slope in the coarse sand to granule range marks the changeover to infiltration-dominated beach hydrodynamics. Average slopes for gravel beaches increase consistently, although gradually, through the pebble and cobble ranges.

8.4. Things become complicated in the cobble to boulder range

From sand through pebbles, the main difference among the beaches is their grain size. But in the cobble and boulder size range, there are two kinds of coastal accumulations: ‘standard’ coarse-clastic beaches, that extend unbroken from the subtidal to the uppermost berm (Fig. 1, bottom; Fig. 3, top); and supratidal coastal boulder deposits forming boulder ridges (Fig. 3, bottom), which are separated from the ocean by bare bedrock surfaces (except during storms). These two types have different slope/clast-size characteristics (Fig. 6): boulder ridges, despite being detached from the fair-weather shoreline, have frontal slopes lying along the expected continuation of the slope/size curve;

but the slopes for boulder beaches are less steep than would be predicted by extrapolation from the pebble and cobble data.

8.4.1. Boulder ridges may be the storm beaches of high-energy exposed coasts

Boulder ridges fall along the main data trend (Fig. 6), suggesting that their steep fronts represent equilibrium faces constructed under strong swash asymmetry. The openness of the clast framework (Fig. 3, bottom) means that infiltration is extreme, so materials brought to the back of the shore platform by wave-generated bores tend to remain there, the incident energy of the uprush having been dissipated by flow thinning, expansion, and infiltration (Buscombe and Masselink, 2006). Clasts can be added to the toe of the existing ridge, or may be transported up the ridge face (Cox et al., 2018).

Both the horizontal distance and the height to which constituent boulders can be transported are related to wave power and storm intensity (Lorang, 2011), although the sedimentologic details are not known. The slope/size data here, however, suggest that boulder ridges may be true storm beaches, albeit detached from the fair-weather shoreline.

8.4.2. Boulder beaches slopes are anomalously gentle

All boulder beaches reported have slopes less than 0.27 (15°) (Fig. 6). Furthermore, the average boulder-beach steepness appears to decrease with increasing grain size (Figs. 6, 7). This tendency was first observed by Oak (1984), who reported that sites in Australia had lower gradients than expected. She hypothesised that boulder beaches were unlikely to have steep slopes because the storm waves that activate them would promote development of flatter profiles, by analogy with storm levelling of sandy beaches (e.g., Komar, 1998; Lee et al., 1995; Wang et al., 2006). However, the steep equilibrium slopes of boulder ridges, discussed above, indicate that this is not necessarily the case. In addition, Masselink and Puleo (2006) argue that storm flattening of beaches results not from dynamical differences between storm and fair-weather waves, but because higher water levels due to wave setup mean that parts of the beach built by swash processes are in the surf zone during storms, and thus subject to breaking waves and strong return flows.

Beach-face reorganisation requires waves capable of transporting all the available clasts, across the full range of sizes: this means not only that individual waves must be that powerful, but that there have to be enough of them to complete the work for the entire beach. In the case of boulder beaches, it may be that few storms can produce a sufficient number of waves with the requisite power. Piecemeal activation, in addition to the armouring effect of in-situ jostling by lower-energy swash, may contribute to the overall lower slopes that characterise boulder beaches. But whether the trend of decreasing beach-face slope with increasing clast size for boulder beaches is true in general cannot be determined from the limited measurements available: populations with median size > 128 mm make up less than 2% of the data (only 33 points of the 2144 on Fig. 6).

8.4.3. Caveats and red flags

It's important to bear two things in mind when interpreting the apparent geomorphological differences among the boulder ridge and boulder beach data. First, this region of the parameter space is the most thinly populated, with only 35 data points in the coarse-cobble range, and only 33 across fine and medium boulders: in aggregate, just 5% of the total data set. Thus, trends in this region are inherently statistically insignificant.

Second, among the studies of cobble and boulder deposits, there are large differences in size-counting methodologies. Studies of boulder beaches often focus on the largest clasts, so reported medians may be skewed toward the coarser fraction (see e.g. the different approaches of Chen et al., 2011; Etienne and Paris, 2010; Oak, 1981; Pérez-Alberti et al., 2012; Zentner, 2009). This hinders comparisons among the

studies. For example, the data for boulder beaches (which are from just three studies: Oak, 1981; Etienne and Paris, 2010; and Pérez-Alberti et al., 2012) were collected using methods unlikely to capture the full size spectrum. The Oak (1981) data come from the surface layer of the beach (which excludes smaller clasts that have migrated into interstitial spaces), Etienne and Paris (2010) measured sets of contiguous boulders; and Pérez-Alberti and Trenhaile (2015b) conducted hand-digitised clast counts that excluded smaller cobbles and finer grains (see their Fig. 6). In contrast, the boulder ridge data (Jahn, 2014; Zentner, 2009) were collected by ribbon counting, which explicitly included every clast on the transect, whether or not it lay at the surface. Thus medians for the boulder ridge studies approximate the medians for the size population as a whole, whereas the boulder beach data represent the coarser fraction.

The point here is not to criticise one study relative to another, but to illustrate the problem of methodological variability inherent in meta-analyses. When there are copious studies (as in the case of sandy beaches), the specific measurement procedures are less important, as the sheer volume of data will average out the variations. But with so few studies of coarser beaches, and given that it is more difficult to compile random, statistically significant grain size data from cobble- and boulder-dominated deposits, differences among studies can influence the apparent trends. More sedimentologic data from both boulder ridges and boulder beaches are required to characterise the slope/grain-size relationships in this complex set of environments.

8.4.4. Caveats aside, there appear to be consistent differences among boulder ridges and boulder beaches

Although the slope/size characteristics of coarse cobble and boulder deposits are not well constrained by this data set—which raises more questions in these size categories than it answers—the consistency of the segregation between boulder ridges and boulder beaches suggests real hydrodynamic differences. No boulder beaches have faces steeper than 0.27 ($\sim 15^\circ$), whereas most boulder ridges have gradients in excess of that, and ranging up to almost twice as much ($\tan \beta = 0.48$, $\sim 27^\circ$).

Boulder ridges are not reached by fair weather waves, nor even by regular storms: they experience only the highest wave power. This means that all waves reaching the ridge have the power to transport the constituent clasts, and the result is an equilibrium face, reflecting the very strong swash asymmetry expected in these coarse, exceedingly permeable clast piles. Boulder beaches, in contrast, are subject to tidal inflow and outflow, and are constantly lapped by low and medium energy waves. These more gentle processes are not competent to transport most of the constituent clasts, but by jostling particles in situ, may tend to promote closer packing and armouring of the surface (Oak, 1981). Boulder ridges are never subject to this kind of low-level re-organisation. It is possible—but not demonstrated—that this is one of the key dynamical differences between boulder ridges and boulder beaches. The bottom line, however, is that much work remains to be done on these environments.

8.5. The grain-size/slope trends and equation

Despite the complexities in the cobble and boulder size regions, and despite the wide array of studies and methodologies in the compiled studies, the data set has a remarkably coherent story to tell. The steep grain-size/slope relationships in the sand realm contrast with the gentler—but still distinct—trend across the coarser size grades. The change in slope can be related to known dynamics, and its location helps refine understanding of grain size thresholds for those processes. In addition, the differing grain-size/slope characteristics for boulder ridges and boulder beaches opens a window into these relatively unexamined environments.

Eq. (2) provides a semi-quantitative framework to describe the broad patterns in the data set. Clearly the predictive power of this expression is low: the data integrate across many different settings and

conditions, and consequently there is lots of noise and scatter. Moreover, grain size is but one of the many variables that contribute to beach face slope. Grain size goes hand-in-hand with sorting and hydraulic conductivity; but also important are grain density and grain shape. The latter in particular, by controlling the angle of internal friction, can play a strong role in determining equilibrium slope. There are numerous hydrodynamic factors that will exert local control on beach shape—including the height, period, and prevailing wave approach angle—and these will depend on the local wave climate and topography. Tide range is also an important factor in controlling the width of the swash zone and the effectiveness of wave attack at various levels. Finally, the temporal effects of sediment budget and net energy, governing whether the beach is in a state of net accretion or net erosion, will also impact slope. And all of these are inter-related, and as they also control grain size, they relate to slope in multiple ways. The unified grain-size/slope equation (Eq. 2) therefore cannot and should not be used to make categoric statements about grain-size/slope relationships.

This equation can, however, serve as the basis for a more general understanding of the first-order behaviour of loose sediment along coastlines. It formalises the general relationship between beach-face slope and grain size over several orders of magnitude; and most importantly it describes the changes in the relationship at coarser size grades. Thus the equation may help frame future research questions and drive better understanding of questions—many of which are still unanswered (Komar and Sunamura, 2015)—regarding the relative importance of grain transport processes in beach geomorphology.

9. Conclusions

The present analysis provides a comprehensive picture of trends in beach-face slope across the full spectrum of grain sizes and a universal equation relating the slope of the beach face to the size of its sediment. This is a substantial advance on previous studies, which produced simple straight-line relationships in log-log space, based on a limited (and fine) size range. Compiling data over the whole range of sediment sizes encountered in the coastal environment reveals that such formulae cannot account for all the variability of the slope-size relationship. The new formula (Eq. 2) describes both the large steepness increase in the finer sand sizes and the change to a more gentle increase in coarse sand and gravel beaches (Fig. 9).

The paucity of data for the coarser grain sizes (Fig. 6) dramatically illustrates the extraordinary emphasis that has been placed on sandy coasts. Although this can be understood from a socio-economic perspective, it skews our understanding of beach systems as a whole. A better understanding of coarse clast beaches is relevant to coastal engineering, because restored or nourished beach faces that are too steeply engineered are inevitably ‘recalled’ to milder values (Anfuso et al., 2001; Phillips, 1985; Seymour et al., 2005). And a better understanding of the slope characteristics of cobble and boulder beaches would be a particular advantage in development of coarse revetments in high-energy settings (Allan et al., 2006; Komar, 2007; Stripling et al., 2008).

The data distribution (Figs. 6, 7, 9) graphically confirms the significance of changes related to evolving hydrodynamics as beaches transition from being relatively impermeable—with grain transport strongly controlled by effective weight modification (below 0.3 mm) and boundary layer thickness (around 0.5 mm)—to having increasingly good hydraulic conductivity (above 1.5 mm). The increasing importance of infiltration dominated dynamics in coarser beaches leads to depositional mechanics that are controlled by the level of swash asymmetry. That the data set illustrates this changeover, and also shows its grain size dependency being more subtle than the slope effects in finer sizes, is a new and interesting result.

Finally, this data set gives new perspective on the coarsest deposits: boulder beaches and boulder ridges. The dynamics in these two environments—the one washed constantly by waves of varying energy,

the other fully isolated from the ocean except in the case of the strongest storms—are not fully understood. The amalgamated data support previous observations (Oak, 1984) that boulder beaches tend to have lower slopes than cobble beaches, although the data remain statistically inadequate to prove this. The data also show that boulder ridges plot along the main data trend, with steeper average slopes than cobble or pebble beaches, supporting the argument that they should be considered supratidal storm beaches on very high-energy coasts.

Data availability

The data set of size/slope values related to this article, and the details of the references they were extracted from, can be found at <https://doi.org/10.5281/zenodo.3241984>, hosted by Zenodo (Bujan et al., 2018b).

Declaration of competing interest

None.

Acknowledgments

Nans Bujan thanks the Ministry of Science and Technology of Taiwan for financial support [grant number 106-2911-I-006-301]. Rónadh Cox acknowledges support from National Science Foundation awards 0921962 and 1529756. Fieldwork support was provided by Wen-Son Chiang and his team (Tainan Hydraulics Laboratory). We are also grateful to Nobuhisa Kobayashi for his helpful comments. Some of the data presented was kindly provided by Cyprien Bosscherelle, Jorge Guillen, Alex Horner-Devine, Nicolas Aleman, Celso Pinto, Jonathan Fram, Jon Miller, Thierry Garlan, Tanya Silveira, Augusto Pérez-Alberti, Alan Trenhaile, Ian Miller, Jon Kemp, Samuel Etienne, Raphaël Paris and members of the ‘Coastal List’ community (http://www.coastal.udel.edu/coastal/coastal_list.html). An anonymous referee is acknowledged for his comments that helped to improve the manuscript.

References

- Aagaard, T., Hughes, M., Baldock, T., Greenwood, B., Kroon, A., Power, H., 2012. Sediment transport processes and morphodynamics on a reflective beach under storm and non-storm conditions. *Mar. Geol.* 326–328, 154–165. <https://doi.org/10.1016/j.margeo.2012.09.004>. oct.
- Allan, C.J., Geitgey, R.P., Hart, R., 2005. Dynamic Revetments for Coastal Erosion in Oregon. Oregon Department of Transportation, Newport, OR, United States. <https://digital.osl.state.or.us/islandora/object/osl:10470>.
- Allan, J.C., Hart, R., Tranquili, J.V., 2006. The use of passive integrated transponder (PIT) tags to trace cobble transport in a mixed sand-and-gravel beach on the high-energy Oregon coast, USA. *Mar. Geol.* 232 (1–2), 63–86. <https://doi.org/10.1016/j.margeo.2006.07.005>. oct.
- Almeida, L.P., Masselink, G., Russell, P., Davidson, M., McCall, R., Poate, T., 2014. Swash zone morphodynamics of coarse-grained beaches during energetic wave conditions. In: *Coastal Engineering Proceedings*. 1. pp. 35 oct.
- Almeida, L.P., Masselink, G., Russell, P.E., Davidson, M., Poate, T., McCall, R., Blenkinsopp, C., Turner, I.L., 2013. Observations of the Swash Zone on a Gravel Beach During a Storm Using a Laser-Scanner (Lidar). apr. SI 65. *Journal of Coastal Research*, Plymouth, England, pp. 636–641.
- Anfuso, G., Benavente, J., Gracia, F.J., 2001. Morphodynamic responses of nourished beaches in SW Spain. *J. Coast. Conserv.* 7 (1), 71–80. <https://doi.org/10.1007/BF02742469>. mar.
- Anfuso, G., del Pozo, J.A.M., Nachite, D., Benavente, J., Macias, A., 2007. Morphological characteristics and medium-term evolution of the beaches between Ceuta and Cabo Negro (Morocco). *Environ. Geol.* 52 (5), 933–946. <https://doi.org/10.1007/s00254-006-0535-3>. may.
- Aragonés, L., López, I., Villacampa, Y., Serra, J., Saval, J., 2015. New methodology for the classification of gravel beaches: adjusted on Alicante (Spain). *J. Coast. Res.* 31 (4), 1023–1034. <https://doi.org/10.2112/JCOASTRES-D-14-00140.1>.
- Autret, R., Suárez, S., Fichaut, B., Etienne, S., 2016. Elaboration d'une typologie des dépôts de blocs supratidiaux des sommets de falaise de la péninsule de Reykjanes (Islande). Géomorphologie : relief, processus, environnement 22 (1), 61–76. <https://doi.org/10.4000/géomorphologie.11272>. apr.
- Bagnold, R.A., 1940. Beach formation by waves: some model experiments in a wave tank. (Includes photographs). *Journal of the Institution of Civil Engineers* 15 (1), 27–52. <https://doi.org/10.1680/ijoti.1940.14279>. nov.
- Bascom, W.N., 1951. The relationship between sand size and beach-face slope. *Eos Trans. AGU* 32 (6), 866–874. <https://doi.org/10.1029/TR032i006p00866>.
- Battjes, J., 1974. Surf Similarity. In: *Coastal Engineering 1974*. American Society of Civil Engineers, Copenhagen, Denmark, pp. 466–480 jun.
- Bertoni, D., Grottoli, E., Ciavola, P., Sarti, G., Benelli, G., Pozzebon, A., 2013. On the displacement of marked pebbles on two coarse-clastic beaches during short fair-weather periods (Marina di Pisa and Portonovo, Italy). *Geo-Mar. Lett.* 33 (6), 463–476. <https://doi.org/10.1007/s00367-013-0341-3>. dec.
- Bird, E.C.F., 2011. *Coastal Geomorphology: An Introduction*. sep. John Wiley & Sons.
- Blenkinsopp, C.E., Turner, I.L., Masselink, G., Russell, P.E., 2011. Swash zone sediment fluxes: field observations. *Coast. Eng.* 58 (1), 28–44. <https://doi.org/10.1016/j.coastaleng.2010.08.002>. jan.
- Bluck, B.J., 1998. Clast assembling, bed-forms and structure in gravel beaches. *Earth Environ. Sci. Trans. R. Soc. Edinb.* 89 (4), 291–323. <https://doi.org/10.1017/S026359330000242X>. jan.
- Boon, J.D., Green, M.O., 1988. Caribbean Beach-face Slopes and Beach Equilibrium Profiles. 1. *Coastal Engineering Proceedings*, Torremolinos, Spain, pp. 1618–1630.
- Borzone, C.A., Rosa, L.C., 2009. Impact of oil spill and posterior clean-up activities on wrack-living talitrid amphipods on estuarine beaches. *Braz. J. Oceanogr.* 57 (4), 315–323. <https://doi.org/10.1590/S1679-87592009000400006>. dec.
- Bujan, N., Cox, R., Lin, L.-C., Ducrocq, C., Hwung, H.-H., 2018a. Semiautomatic digital clast sizing of a Cobble Beach, Nantian, Taiwan. *J. Coast. Res.* 34 (6), 1367–1381. <https://doi.org/10.2112/JCOASTRES-D-17-00165.1>. feb.
- Bujan, N., Cox, R., Masselink, G., 2018b. From fine sand to boulders: examining the relationship between beach-face slope and sediment size. Dataset and references. <https://doi.org/10.5281/zenodo.3241984>.
- Buscombe, D., Masselink, G., 2006. Concepts in gravel beach dynamics. *Earth Sci. Rev.* 79 (1–2), 33–52. <https://doi.org/10.1016/j.earscirev.2006.06.003>. nov.
- Butt, T., Russell, P., Turner, I., 2001. The influence of swash infiltration-exfiltration on beach face sediment transport: onshore or offshore? *Coast. Eng.* 42 (1), 35–52. [https://doi.org/10.1016/S0378-3839\(00\)00046-6](https://doi.org/10.1016/S0378-3839(00)00046-6). jan.
- Carr, A.P., 1969. Size grading along a pebble beach; Chesil Beach, England. *J. Sediment. Res.* 39 (1), 297–311. <https://doi.org/10.1306/74D71C3A-2B21-11D7-8648000102C1865D>. jan.
- Carter, R.W.G., Orford, J.D., 1993. The morphodynamics of coarse clastic beaches and barriers: a short- and long-term perspective. *J. Coast. Res.* SI (15), 158–179. <http://www.jstor.org/stable/25735728> apr.
- Chen, B., Chen, Z., Stephenson, W., Finlayson, B., 2011. Morphodynamics of a boulder beach, Putuo Island, SE China coast: the role of storms and typhoon. *Mar. Geol.* 283 (1–4), 106–115. <https://doi.org/10.1016/j.margeo.2010.10.004>. may.
- Cox, R., Jahn, K.L., Watkins, O.G., Cox, P., 2018. Extraordinary boulder transport by storm waves (west of Ireland, Winter 2013–2014), and criteria for analysing coastal boulder deposits. *Earth Sci. Rev.* 177, 623–636. <https://doi.org/10.1016/j.earscirev.2017.12.014>. feb.
- Cox, R., Lopes, W.A., Jahn, K.L., 2017. Roundness measurements in coastal boulder deposits. *Mar. Geol.* <https://doi.org/10.1016/j.margeo.2017.03.003>.
- Cox, R., Zentner, D., Kirchner, B., Cook, M., 2012. Boulder ridges on the Aran Islands (Ireland): recent movements caused by storm waves, not tsunamis. *J. Geol.* 120 (3), 249–272. <https://doi.org/10.1086/664787>.
- Dail, H.J., Merrifield, M.A., Bevis, M., 2000. Steep beach morphology changes due to energetic wave forcing. *Mar. Geol.* 162 (2–4), 443–458. [https://doi.org/10.1016/S0025-3227\(99\)00072-9](https://doi.org/10.1016/S0025-3227(99)00072-9). jan.
- Deguara, J.C., Gauci, R., 2017. Evidence of extreme wave events from boulder deposits on the south-east coast of Malta (Central Mediterranean). *Nat. Hazards* 86 (2), 543–568. <https://doi.org/10.1007/s11069-016-2525-4>. apr.
- Dubois, R.N., 1972. Inverse Relation between foreshore slope and mean grain size as a function of the heavy mineral content. *Geol. Soc. Am. Bull.* 83 (3), 871–876. [https://doi.org/10.1130/0016-7606\(1972\)83\[871:IRFSAS\]2.0.CO;2](https://doi.org/10.1130/0016-7606(1972)83[871:IRFSAS]2.0.CO;2). jan.
- Elfrink, B., Baldoek, T., 2002. Hydrodynamics and sediment transport in the swash zone: a review and perspectives. *Coast. Eng.* 45 (3–4), 149–167. [https://doi.org/10.1016/S0378-3839\(02\)00032-7](https://doi.org/10.1016/S0378-3839(02)00032-7). may.
- Etienne, S., Paris, R., 2010. Boulder accumulations related to storms on the south coast of the Reykjanes Peninsula (Iceland). *Geomorphology* 114 (1–2), 55–70. <https://doi.org/10.1016/j.geomorph.2009.02.008>.
- Flemming, B.W., 2011. 3.02 – geology, morphology, and sedimentology of estuaries and coasts. In: *Treatise on Estuarine and Coastal Science*. Academic Press, Waltham, pp. 7–38.
- Gopalakrishnan, S., Smith, M.D., Slott, J.M., Murray, A.B., 2011. The value of disappearing beaches: a hedonic pricing model with endogenous beach width. *J. Environ. Econ. Manag.* 61 (3), 297–310. <https://doi.org/10.1016/j.jeem.2010.09.003>. may.
- Graham, D.J., Rollet, A.-J., Rice, S.P., Piégay, H., 2012. Conversions of surface grain-size samples collected and recorded using different procedures. *J. Hydraul. Eng.* 138 (10), 839–849. [https://doi.org/10.1061/\(ASCE\)HY.1943-7900.0000595](https://doi.org/10.1061/(ASCE)HY.1943-7900.0000595).
- Guza, R.T., Inman, D.L., 1975. Edge waves and beach cusps. *J. Geophys. Res.* 80 (21), 2997–3012. <https://doi.org/10.1029/JC080i021p02997>. jul.
- Hall, A.M., Hansom, J.D., Williams, D.M., Jarvis, J., 2006. Distribution, geomorphology and lithofacies of cliff-top storm deposits: examples from the high-energy coasts of Scotland and Ireland. *Mar. Geol.* 232 (3–4), 131–155. <https://doi.org/10.1016/j.margeo.2006.06.008>.
- Hansom, J.D., Barltrop, N.D.P., Hall, A.M., 2008. Modelling the processes of cliff-top erosion and deposition under extreme storm waves. *Mar. Geol.* 253 (1–2), 36–50. <https://doi.org/10.1016/j.margeo.2008.02.015>. jul.
- Hansom, J.D., Hall, A.M., 2009. Magnitude and frequency of extra-tropical North Atlantic cyclones: a chronology from cliff-top storm deposits. *Quat. Int.* 195 (1), 42–52. <https://doi.org/10.1016/j.quaint.2007.11.010>. feb.
- Hansom, J.D., Switzer, A.D., Pile, J., 2015. Chapter 11 - extreme waves: causes,

- characteristics, and impact on coastal environments and society. In: Shroder, J.F., Ellis, J.T., Sherman, D.J. (Eds.), *Coastal and Marine Hazards, Risks, and Disasters*. Elsevier, Boston, pp. 307–334. <https://www.sciencedirect.com/science/article/pii/B978012396483000011X>.
- Hartmann, D., 1991. Cross-shore selective sorting processes and grain size distributional shape. In: Barndorff-Nielsen, Prof Ole E., Willetts, P.B.B. (Eds.), *Aeolian Grain Transport*. Acta Mechanica Supplementum. Springer Vienna, pp. 49–63. http://link.springer.com/chapter/10.1007/978-3-7091-6703-8_4.
- Hoffmann, G., Reicherter, K., Wiatr, T., Grützner, C., Rausch, T., 2013. Block and boulder accumulations along the coastline between Fins and Sur (Sultanate of Oman): tsunamiogenic remains? *Nat. Hazards* 65 (1), 851–873. <https://doi.org/10.1007/s11069-012-0399-7>.
- Holland, K.T., Elmore, P.A., 2008. A review of heterogeneous sediments in coastal environments. *Earth Sci. Rev.* 89 (3–4), 116–134. <https://doi.org/10.1016/j.earscirev.2008.03.003>. aug.
- Hoque, M.A., Asano, T., 2007. Numerical study on wave-induced filtration flow across the beach face and its effects on swash zone sediment transport. *Ocean Eng.* 34 (14–15), 2033–2044. <https://doi.org/10.1016/j.oceaneng.2007.02.004>. oct.
- Horn, D.P., 2006. Measurements and modelling of beach groundwater flow in the swash-zone: a review. *Cont. Shelf Res.* 26 (5), 622–652. <https://doi.org/10.1016/j.csr.2006.02.001>. apr.
- Isla, F.I., Bujalesky, G.G., 2005. Groundwater dynamics on macrotidal gravel beaches of Tierra del Fuego, Argentina. *J. Coast. Res.* 21 (1), 65–72. <https://doi.org/10.2112/02102.1>.
- Ivamy, M.C., Kench, P.S., 2006. Hydrodynamics and morphological adjustment of a mixed sand and gravel beach. *Torre, Bay or Plenty, New Zealand. Mar. Geol.* 228 (1–4), 137–152. <https://doi.org/10.1016/j.margeo.2006.01.002>. apr.
- Jahn, K.L., 2014. The Sedimentology of Storm-Emplaced Coastal Boulder Deposits in the Northeastern Atlantic Region. B.S. Thesis. Williams College, Williamstown, USA. <https://unbound.williams.edu/theses/islandora/object/studenttheses582>.
- Jennings, R., Shulmeister, J., 2002. A field based classification scheme for gravel beaches. *Mar. Geol.* 186 (3–4), 211–228. [https://doi.org/10.1016/S0025-3227\(02\)00314-6](https://doi.org/10.1016/S0025-3227(02)00314-6). jul.
- Karambas, T.V., 2003. Modelling of infiltration-exfiltration effects of cross-shore sediment transport in the swash zone. *Coast. Eng. J.* 45 (01), 63–82. <https://doi.org/10.1142/S057856340300066X>. mar.
- Karsten, M., 2017. Shoreline Management Guidelines. DHI Water and Environment, Horsholm Denmark. https://www.dhigroup.com/upload/campaigns/shoreline/assets/ShorelineManagementGuidelines_Feb2017-TOC.pdf.
- Karunaratna, H., Horrillo-Caraballo, J.M., Ranasinghe, R., Short, A.D., Reeve, D.E., 2012. An analysis of the cross-shore beach morphodynamics of a sandy and a composite gravel beach. *Mar. Geol.* 299–302, 33–42. <https://doi.org/10.1016/j.margeo.2011.12.011>. mar.
- Kennedy, A.B., Mori, N., Yasuda, T., Shimozono, T., Tomiczek, T., Donahue, A., Shimura, T., Imai, Y., 2017. Extreme block and boulder transport along a cliffted coastline (Calicoan Island, Philippines) during Super Typhoon Haiyan. *Mar. Geol.* 383, 65–77. <https://doi.org/10.1016/j.margeo.2016.11.004>. jan.
- Kim, H., Hall, K., Jin, J.-Y., Park, G.-S., Lee, J., 2014. Empirical estimation of beach-face slope and its use for warning of berm erosion. *Journal of Measurements in Engineering* 2 (1), 29–42. <http://www.jve.lt/Vibro/JME-2014-2-1/JME00214030039.html> mar.
- Komar, P.D., 1998. *Beach Processes and Sedimentation*, second. Prentice-Hall, Englewood-Cliffs.
- Komar, P.D., 2007. The design of stable and aesthetic beach fills: learning from nature. In: *Coastal Sediments '07*. American Society of Civil Engineers, New Orleans, Louisiana, United States, pp. 420–433.
- Komar, P.D., Sunamura, T., 2015. Morphology of erosional and accretionary coasts. In: International Compendium of Coastal Engineering. WORLD SCIENTIFIC, pp. 153–195. https://www.worldscientific.com/doi/abs/10.1142/9789814449434_0005.
- Lee, G.-h., Nicholls, R.J., Birkemeier, W.A., Leatherman, S.P., 1995. A conceptual fair-weather-storm model of beach nearshore profile evolution at Duck, North Carolina, U.S.A. *J. Coast. Res.* 11 (4), 1157–1166. <https://www.jstor.org/stable/4298419>.
- Lorang, M.S., 2000. Predicting threshold entrainment mass for a boulder beach. *J. Coast. Res.* 16 (2), 432–445. <http://www.jstor.org/stable/4300052> apr.
- Lorang, M.S., 2011. A wave-competence approach to distinguish between boulder and megaclast deposits due to storm waves versus tsunamis. *Mar. Geol.* 283 (1), 90–97. <https://doi.org/10.1016/j.margeo.2010.10.005>. may.
- Masselink, G., Li, L., 2001. The role of swash infiltration in determining the beachface gradient: a numerical study. *Mar. Geol.* 176 (1–4), 139–156. [https://doi.org/10.1016/S0025-3227\(01\)00161-X](https://doi.org/10.1016/S0025-3227(01)00161-X). jun.
- Masselink, G., Puleo, J.A., 2006. Swash-zone morphodynamics. *Cont. Shelf Res.* 26 (5), 661–680. <https://doi.org/10.1016/j.csr.2006.01.015>. apr.
- Masselink, G., Russell, P., Blenkinsopp, C., Turner, I., 2010. Swash zone sediment transport, step dynamics and morphological response on a gravel beach. *Mar. Geol.* 274 (1–4), 50–68. <https://doi.org/10.1016/j.margeo.2010.03.005>. aug.
- Masselink, G., Russell, P., Turner, I., Blenkinsopp, C., 2009. Net sediment transport and morphological change in the swash zone of a high-energy sandy beach from swash event to tidal cycle time scales. *Mar. Geol.* 267 (1–2), 18–35. <https://doi.org/10.1016/j.margeo.2009.09.003>. nov.
- Masselink, G., Short, A.D., 1993. The effect of tide range on beach morphodynamics and morphology: a conceptual beach model. *J. Coast. Res.* 9 (3), 785–800. <http://www.jstor.org/stable/4298129>.
- McGlashan, D.J., Duck, R.W., Reid, C.T., 2005. Defining the foreshore: coastal geomorphology and British laws. *Estuar. Coast. Shelf Sci.* 62 (1), 183–192. <https://doi.org/10.1016/j.ecss.2004.08.016>.
- McKay, P.J., Terich, T.A., 1992. Gravel barrier morphology: Olympic National Park, Washington State, USA. *J. Coast. Res.* 8 (4), 813–829. <http://www.jstor.org/stable/4298038>.
- McLachlan, A., Dorvlo, A., 2005. Global patterns in sandy beach macrobenthic communities. *J. Coast. Res.* 21 (4), 674–687. <https://doi.org/10.2112/03-0114.1>. jul.
- McLean, R.F., Kirk, R.M., 1969. Relationships between grain size, size-sorting, and fore-shore slope on mixed sand - shingle beaches. *N. Z. J. Geol. Geophys.* 12 (1), 138–155. <https://doi.org/10.1080/00288306.1969.10420231>. may.
- Morton, R.A., Richmond, B.M., Jaffe, B.E., Gelfenbaum, G., 2008. Coarse-clast ridge complexes of the Caribbean: a preliminary basis for distinguishing tsunami and storm-wave origins. *J. Sediment. Res.* 78 (9), 624–637. <https://doi.org/10.2110/jsr.2008.068>. jan.
- Morton, R.A., Speed, F.M., 1998. Evaluation of shorelines and legal boundaries controlled by water levels on sandy beaches. *J. Coast. Res.* 14 (4), 1373–1384. <http://www.jstor.org/stable/4298899>.
- Mwakumanya, M.A., Bdo, O., 2007. Beach morphological dynamics: a case study of Nyali and Bamburi Beaches in Mombasa, Kenya. *J. Coast. Res.* 232, 374–379. <https://doi.org/10.2112/04-0354.1>. mar.
- Nielsen, P., 1998. Coastal groundwater dynamics. In: *Coastal Dynamics '97*. ASCE, Plymouth, pp. 546–555. <http://cedb.asce.org/CEDBsearch/record.jsp?dockey=0111142>.
- Nott, J., 2003. Waves, coastal boulder deposits and the importance of the pre-transport setting. *Earth Planet. Sci. Lett.* 210 (1–2), 269–276. [https://doi.org/10.1016/S0012-821X\(03\)00104-3](https://doi.org/10.1016/S0012-821X(03)00104-3). may.
- Oak, H.L., 1981. Boulder Beaches: A Sedimentological Study. Ph.D. Macquarie University, Sydney, Australia. <http://minerva.mq.edu.au:8080/vital/access/manager/Repository/mq:9268>.
- Oak, H.L., 1984. The boulder beach: a fundamentally distinct sedimentary assemblage. *Ann. Assoc. Am. Geogr.* 74 (1), 71–82. <https://doi.org/10.1111/j.1467-8306.1984.tb01435.x>. mar.
- Packwood, A.R., 1983. The influence of beach porosity on wave uprush and backwash. *Coast. Eng.* 7 (1), 29–40. [https://doi.org/10.1016/0378-3839\(83\)90025-X](https://doi.org/10.1016/0378-3839(83)90025-X). feb.
- Paris, R., Naylor, L.A., Stephenson, W.J., 2011. Boulders as a signature of storms on rock coasts. *Mar. Geol.* 283 (1–4), 1–11. <https://doi.org/10.1016/j.margeo.2011.03.016>. may.
- Pérez-Alberti, A., Trenhaile, A.S., 2015. Clast mobility within boulder beaches over two winters in Galicia, northwestern Spain. *Geomorphology* 248, 411–426. <https://doi.org/10.1016/j.geomorph.2015.08.001>. nov.
- Pérez-Alberti, A., Trenhaile, A.S., 2015. An initial evaluation of drone-based monitoring of boulder beaches in Galicia, north-western Spain: drone-based monitoring. *Earth Surf. Process. Landf.* 40 (1), 105–111. <https://doi.org/10.1002/esp.3654>. jan.
- Pérez-Alberti, A., Trenhaile, A.S., Pires, A., López-Bedoya, J., Chamíné, H.I., Gomes, A., 2012. The effect of boulders on shore platform development and morphology in Galicia, north west Spain. *Cont. Shelf Res.* 48, 122–137. <https://doi.org/10.1016/j.csr.2012.07.014>. oct.
- Phillips, J.D., 1985. Headland-bay beaches revisited: an example from Sandy Hook, New Jersey. *Mar. Geol.* 65 (1), 21–31. [https://doi.org/10.1016/0025-3227\(85\)90044-1](https://doi.org/10.1016/0025-3227(85)90044-1). may.
- Phillips, M.R., House, C., 2009. An evaluation of priorities for beach tourism: case studies from South Wales, UK. *Tour. Manag.* 30 (2), 176–183. <https://doi.org/10.1016/j.tourman.2008.05.012>. apr.
- Pinto, C.A., Taborda, R., Andrade, C., Teixeira, S.B., 2009. Seasonal and mesoscale variations at an Embayed Beach (Armaçao de Pera, Portugal). *J. Coast. Res.* 118–122. <http://www.jstor.org/stable/25737549>.
- Prodrige, S., Russell, P., Davidson, M., Miles, J., Scott, T., 2016. Understanding and predicting the temporal variability of sediment grain size characteristics on high-energy beaches. *Mar. Geol.* 376, 109–117. <https://doi.org/10.1016/j.margeo.2016.04.003>. jun.
- Qi, H., Cai, F., Lei, G., Cao, H., Shi, F., 2010. The response of three main beach types to tropical storms in South China. *Mar. Geol.* 275 (1–4), 244–254. <https://doi.org/10.1016/j.margeo.2010.06.005>. sep.
- Rector, R.L., 1954. *Laboratory Study of Equilibrium Profiles of Beaches. Technical Memorandum. U.S. Army Corps of Engineers*.
- Reis, A.H., Gama, C., 2010. Sand size versus beachface slope—an explanation based on the constructal law. *Geomorphology* 114 (3), 276–283. <https://doi.org/10.1016/j.geomorph.2009.07.008>. jan.
- Reniers, A.J.H.M., Gallagher, E.L., MacMahan, J.H., Brown, J.A., van Rooijen, A.A., van Thiel de Vries, J.S.M., van Prooijen, B.C., 2013. Observations and modeling of steep-beach grain-size variability. *J. Geophys. Res. Oceans* 118 (2), 577–591. <https://doi.org/10.1029/2012JC008073>. feb.
- Roberts, T.M., Wang, P., Puleo, J.A., 2013. Storm-driven cyclic beach morphodynamics of a mixed sand and gravel beach along the Mid-Atlantic Coast, USA. *Mar. Geol.* 346, 403–421. <https://doi.org/10.1016/j.margeo.2013.08.001>. dec.
- Schwartz, M., 2006. *Encyclopedia of Coastal Science*. nov. Springer Science & Business Media. https://link.springer.com/referenceworkentry/10.1007%2F1-4020-3880-1_140.
- Seymour, R., Guza, R.T., O'Reilly, W., Elgar, S., 2005. Rapid erosion of a small southern California beach fill. *Coast. Eng.* 52 (2), 151–158. <https://doi.org/10.1016/j.coastaleng.2004.10.003>. feb.
- Shah-Hosseini, M., Saleem, A., Mahmoud, A.-M.A., Morhange, C., 2016. Coastal boulder deposits attesting to large wave impacts on the Mediterranean coast of Egypt. *Nat. Hazards* 83 (2), 849–865. <https://doi.org/10.1007/s11069-016-2349-2>. may.
- Shepherd, R.G., 1989. Correlations of permeability and grain size. *Ground Water* 27 (5), 633–638. <https://doi.org/10.1111/j.1745-6584.1989.tb00476.x>. sep.
- Silvester, R., Hsu, J.R.C., 1997. *Coastal Stabilization. World Scientific*.
- Soares, A.G., 2003. Sandy Beach Morphodynamics and Macrofaunal Communities in

- Temperate, Subtropical and Tropical Regions: A Macroecological Approach. Ph.D.. University of Port Elizabeth, Port Elizabeth, South Africa. <https://core.ac.uk/download/pdf/145047838.pdf>.
- Stripling, S., Bradbury, A.P., Cope, S.N., Brampton, A.H., 2008. Understanding Barrier Beaches. Technical Report. Department for Environment, Food and Rural Affairs. <http://repository.tudelft.nl/view/hydro/uuid:ff88c128-1221-48f9-9c41-537515741a51/>.
- Sunamura, T., 1975. "Static" relationship among beach slope, sand size, and wave properties. *Geogr. Rev. Jpn* 48 (7), 485–489. https://www.jstage.jst.go.jp/article/grj1925/48/7/48_7_485/_article/-char/ja/.
- Sunamura, T., 1984. Quantitative predictions of beach-face slopes. *GSA Bulletin* 95 (2), 242–245. [https://doi.org/10.1130/0016-7606\(1984\)95<242:QPOBS>2.0.CO;2](https://doi.org/10.1130/0016-7606(1984)95<242:QPOBS>2.0.CO;2). feb.
- Terry, J.P., Goff, J., 2014. Megaclasts: proposed revised nomenclature at the coarse end of the Udden-Wentworth grain-size scale for sedimentary particles. *J. Sediment. Res.* 84 (3), 192–197. <https://doi.org/10.2110/jsr.2014.19>. mar.
- Turner, I.L., Masselink, G., 1998. Swash infiltration-exfiltration and sediment transport. *J. Geophys. Res. Oceans* 103 (C13), 30813–30824. <https://doi.org/10.1029/98JC02606>. dec.
- Turner, I.L., Nielsen, P., 1997. Rapid water table fluctuations within the beach face: implications for swash zone sediment mobility? *Coast. Eng.* 32 (1), 45–59. [https://doi.org/10.1016/S0378-3839\(97\)00015-X](https://doi.org/10.1016/S0378-3839(97)00015-X). oct.
- Vousdoukas, M.I., Wachler, B., Almeida, L.P., Ferreira, O., Alexandrakis, G., Velegrakis, A.F., Schimmels, S., 2013. Predicting beach-face rotation on a meso-tidal, steeply sloping, beach. In: 7th International Conference on Coastal Dynamics, Bordeaux, France, pp. 11. http://www.coastaldynamics2013.fr/pdf_files/175_Vousdoukas_Michalis.pdf.
- Wang, P., Kirby, J.H., Haber, J.D., Horwitz, M.H., Knorr, P.O., Krock, J.R., 2006. Morphological and sedimentological impacts of Hurricane Ivan and immediate poststorm beach recovery along the Northwestern Florida Barrier-Island Coasts. *J. Coast. Res.* 1382–1402. <https://doi.org/10.2112/05-0440.1>. nov.
- Williams, D.M., Hall, A.M., 2004. Cliff-top megaclast deposits of Ireland, a record of extreme waves in the North Atlantic—storms or tsunamis? *Mar. Geol.* 206 (1–4), 101–117. <https://doi.org/10.1016/j.margeo.2004.02.002>. may.
- Wright, L., Short, A., 1984. Morphodynamic variability of surf zones and beaches: a synthesis. *Mar. Geol.* 56 (1–4), 93–118. [https://doi.org/10.1016/0025-3227\(84\)9008-2](https://doi.org/10.1016/0025-3227(84)9008-2).
- Zenkovich, V.P., Zenkovich, V.P., 1967. Processes of Coastal Development. Oliver and Boyd, Edinburgh. [http://agris.fao.org/agris-search/search.do?recordID=\(US201300593254\)](http://agris.fao.org/agris-search/search.do?recordID=(US201300593254)).
- Zentner, D., 2009. Geospatial, Hydrodynamic, and Field Evidence for the Storm-Wave Emplacement of Boulder Ridges on the Aran Islands, Ireland. *Geosciences*. Williams College, Williamstown, USA. <https://unbound.williams.edu/theses/islandora/object/studenttheses%3A492>.